Time Reversal Processing in Ultrasonic Nondestructive Testing

Najet Chakroun, Mathias A. Fink, and François Wu

Abstract— **In this paper, we present a novel and completely different approach to focusing on defects beneath plane or curved surfaces: the time reversal mirror method. The time reversal technique is based on the concept of time reversal of ultrasonic fields and takes into account both the phase and modulus information coming from the defect. This technique is self-adaptative and requires only the presence of a target in the solid sample. In highly scattering media, it is shown that the time reversal process allows a new approach to speckle noise reduction. Experimental results obtained with a 121-channel time reversal mirror on titanium and duralumin samples will be presented. They demonstrate the ability of time reversal to compensate for the distortions induced by liquid–solid interfaces of different geometries and to detect small defects in a noisy background.**

I. Introduction

ULTRASONIC nondestructive testing needs large focusing apertures in order to detect small defects in solid media. Current ultrasonic inspections use scanned immersion techniques. In recent years, two different approaches have been extensively studied in order to obtain focused beams through nonplanar, liquid–solid interfaces. Both techniques require *a priori* knowledge of the geometry of the interface.

In the first technique, the beam focusing is achieved with one or several transducers whose geometry is matched to the liquid–solid interface and to the desired focal point. In this technique, each transducer has a front face designed to equalize all the propagation times between the transducer surface and the desired focal point in the solid. However, due to the curved surfaces, these transducers are in focus for only one point in the solid (with a limited depth of focus). Industrial inspections of thick samples thus require many different transducers.

A greater flexibility can be obtained by the second technique using a multi-element transducer to generate a focal spot in the acoustic beam at any specified angle and range. The 1- and 2-D transducer arrays are connected to a set of electronic delay lines whose values are matched to produce focusing [1]–[3]. The optimal delays, calculated using Snell's law, compensate the propagation time variations between the different elements and the desired focal point. The focusing and beam steering ability result from the interference pattern produced by the delayed acoustic pulses.

These two techniques suffer from important limitations. They are based on an exact *a priori* knowledge of the interface geometry and require highly precise positioning of the transducer. As the transducer aperture becomes larger, the precision of the positioning needs to be higher, and such a precision is not always available in current inspections. Another limitation of this technique is that it assumes that the velocity of sound is known and constant in each propagating medium.

A novel and completely different approach to focusing on defects beneath curved surfaces is presented in this paper. As in the second technique, 1- and 2-D transducer arrays are used. However, neither *a priori* knowledge of the interface geometry is required, nor knowledge of the velocity in the propagating medium. The technique is self-adaptive and only needs the presence of a defect in the sample of interest. It is based on the concept of time reversal of an ultrasonic field that has been developed in our laboratory and applied in the field of medical therapy and medical imaging [4]–[7].

In the time reversal process, we take advantage of the properties of piezoelectric transducers, i.e., their transmit and receive capabilities, their linearity, and the capability for instantaneous measurement of the temporal pressure waveforms. The pressure field $p(\boldsymbol{r}_i, t)$ reflected by a defect is detected with a set of transducer elements located at positions $\boldsymbol{r}_i$ and is digitized and stored during a time interval T. The detected pressure fields are then resynthetized and transmitted by the same transducers in a reversed temporal chronology (last in, first out). This is equivalent to the transmission of $p(\boldsymbol{r}_i, T - t)$. Each transducer of the array is connected to its own electronic circuitry that consists of a receiving amplifier, an A/D converter, a storage memory, and most importantly a programmable transmitter capable of synthesizing a time-reversed version of the stored signals.

Such a Time Reversal Mirror (TRM) can convert a divergent wave issuing from a defect into a convergent wave focusing on it. Unlike an ordinary mirror that produces the virtual image of an acoustic object, the TRM produces a real acoustic image at the position of the initial source. It is a self-focusing technique that compensates geometrical distortions of the array structure as well as those resulting from the propagation through liquid–solid interfaces. It is achieved in real time with simple signal processing; it is a natural focusing process matched to the defect shape and to the geometry of the liquid–solid interface.

Another very attractive feature of time reversal processing is its speckle noise reduction capability. In highly scattering media, the detection of small defects is usually difficult due to the speckle noise generated by the heterogeneous structure. The TRM behaves differently if the echographic signals come from the microstructure or from a defect. If the speckle noise

Manuscript received December 14, 1994; revised July 11, 1995.

The authors are with the Laboratoire Ondes et Acoustique, ESPCI, Université Paris VII, URA C.N.R.S. 1503, 75005 Paris, France.

IEEE Log Number 9414983.

results from a microstructure whose scale is less than the wavelength, the time reversal process cannot refocus on the speckle noise sources due to the loss of information during the propagation. Using this property, we developed a novel signal processing technique that allows one to distinguish, during the inspection, a flaw from high-level incoherent speckle noise.

Experimental results obtained with a 121-channel TRM on titanium and duralumin samples will be presented. They demonstrate the ability of time reversal to compensate the distortions induced by liquid–solid interfaces of different geometries and to detect small defects in a noisy background. Such a self-focusing technique is developed for the detection of defects in industrial applications such as aircraft and engine components.

II. Time-Reversal Through Liquid–Solid Interfaces

The basic theory of the time-reversal process is based on an elementary property of the wave equation in a lossless medium. The wave equation is a partial differential equation where the time derivative appears only at the second order. Indeed, the acoustic pressure field $p(\boldsymbol{r},t)$ satisfies the wave equation in a homogeneous fluid with constant velocity c

$$\frac{1}{c^2}\frac{\partial^2 p}{\partial t^2} = \Delta p. \tag{1}$$

In the case of an isotropic solid immersed in a fluid, the acoustic field is described in the solid by the acoustical displacement $u(\boldsymbol{r},t)$, according to

$$\rho_s \frac{\partial^2 \boldsymbol{u}}{\partial t^2} = (\lambda+2\mu)(\mathbf{grad}\ (div(\boldsymbol{u}))) - \mu(\mathbf{curl}\ (\mathbf{curl}\ (\boldsymbol{u}))) \tag{2}$$

where λ, μ are the Lamé coefficients and ρ_s is the density of the solid.

In (1) and (2), the propagation equation contains only a second-order time-derivative operator. Thus if $p(\boldsymbol{r},t)$ and $u(\boldsymbol{r},t)$ are solutions of (1) and (2), then $p(\boldsymbol{r},-t)$ and $u(\boldsymbol{r},-t)$ are also solutions of the same equations. Moreover, $p(\boldsymbol{r},t)$ in the fluid and $u(\boldsymbol{r},t)$ in the solid are linked by stress and strain continuity at the fluid–solid interface that determine the unique solution $p(\boldsymbol{r},t)$ for the field in the medium. We take advantage of this property to achieve optimal focusing of a pulsed wave on a point-like reflector located in a solid sample immersed in fluid medium. Let $u(\boldsymbol{r},t)$ represent the acoustic displacement in the solid and $p(\boldsymbol{r},t)$ the resulting pressure field in the fluid that propagates from a single point source located in a solid. The optimal way to focus on this source consists of a time reversal of the pressure field in the whole 3-D volume, generating $p(\boldsymbol{r},-t)$ in the fluid, and thus $u(\boldsymbol{r},-t)$ in the solid (Fig. 1). Using Huyghen's principle, we reduce the time reversal operation from a 3-D volume to a 2-D closed surface, resulting in the concept of a closed time reversal cavity [8]. However, a closed cavity is difficult to realize experimentally. A compromise consists of applying the time reversal process to a portion of the cavity, such as a 2-D piezoelectric array located in the fluid medium in front of the solid sample. Such a TRM works as a three-step process. The first step consists in transmitting a pulsed wave to the solid sample from some transducers of the array. The pressure field $p(\boldsymbol{r}_i,t)$ $(1<i<N)$ scattered by a point-like target in the solid sample is then detected with the N elements of the array $\boldsymbol{r}_i$, digitized and recorded within a time interval T. Finally, the pressure field is retransmitted by the same transducers in a reversed temporal chronology (last in, first out). This is equivalent to the transmission of $p(\boldsymbol{r}_i,T-t)$. Such a mirror approximately realizes the backpropagation of the field to its initial source, and thus focuses on the target in the solid.

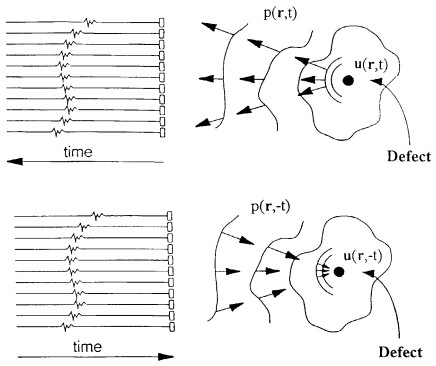

Fig. 1. Time reversal through liquid–solid interface.

The TRM is closely related to the phase conjugation mirror (PCM) developed in Optics. The main difference lies in the fact that time reversal applies to pulsed broadband signals rather than monochromatic ones. Indeed, in contrast to the PCM that works in the continuous wave regime, time reversal processing permits a temporal approach by allowing selection of any time window T that is to be time reversed.

III. Experimental Results in NDT

A. The Prototype

Experimental data on TRM's have been obtained with a real time electronic prototype made of 128 channels working in transmit-receive mode. The transmission module is made of 128 programmable transmitters. Each programmable transmitter is driven by a 32-Kbyte buffer memory through a 12-b D/A converter working at a 40-MHz sampling rate. Each converter is followed by a linear power-amplifier. The transmitter delivers a 30-V peak-to-peak voltage to a 50-Ω transducer impedance. In the transmit mode, the 128 transmitters work simultaneously and are connected to 128 elements of a 2-D transducer array.

Two steps are required in the receive mode: amplification and A/D conversion. We use a set of 16 A/D converters through a multiplexer, so that recording a complete set of A-lines requires eight consecutive emissions. A set of 16 logarithmic amplifiers allows the recording of a 90-dB instantaneous dynamic range through the 16 A/D converters. Recorded data are digitized at a sampling rate of 40 MHz with a 10-b dynamic range. Exponentiation of the data is made in each buffer memory to compensate for the logarithmic operation before time reversal. A PC/AT computer controls the time reversal process and the matching of the dynamic range between the receive and transmit modes. The prototype allows a complete time reversal operation in less than 10 ms and

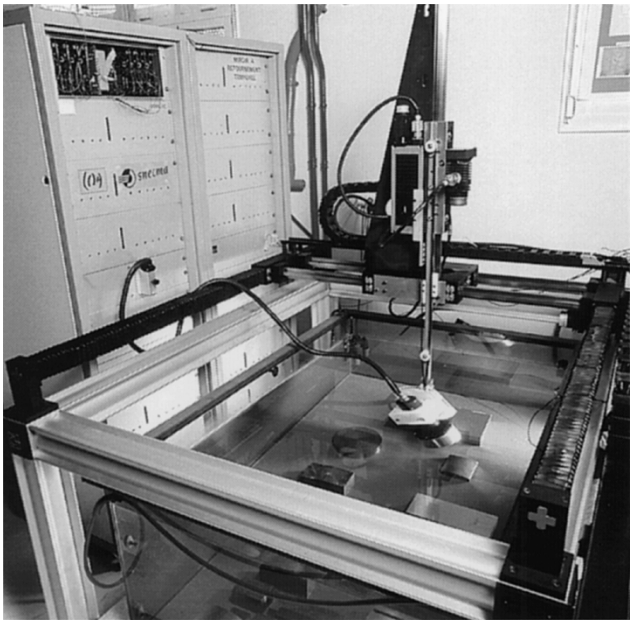

Photo 1.

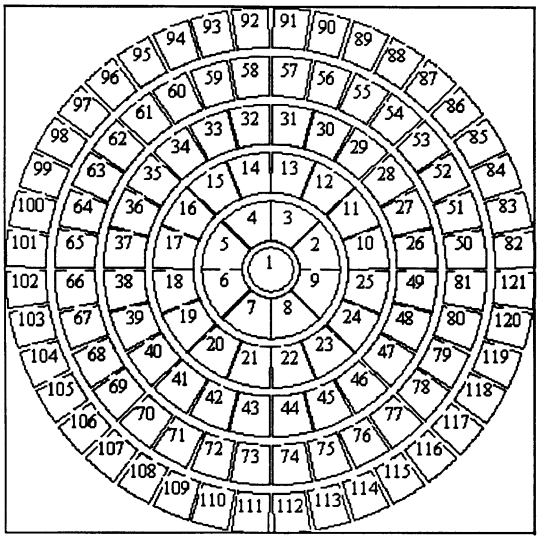

Fig. 2. Two-dimensional transducer array used in time reversal experiments.

different arrays were designed for these experiments (photo 1).

NDT experiments are performed with a 2-D array working at 5 MHz. It is spherically prefocused with a radius of curvature of 330 mm; it contains 121 elements. The central element is a disk of diameter 5 mm and the others are annular sector elements. The transducers are distributed according to a six annuli structure of, respectively, 1, 8, 16, 24, 32, and 40 elements (Fig. 2). Each element of the array is electrically matched to a 50-Ω load with an LC matching network. The total aperture is 60 mm in diameter. The entire titanium block and the 2-D array are immersed in a tank of water.

B. Notations

The complete basic time reversal process requires four steps, two transmit steps and two receive steps. We define some of the notations and basic signal processing in this paper in order to describe simply these steps and also to present the results of the time reversal process.

The signal received on the surface of transducer k at reception step #s is a temporal function $R_{k,s}(t)$. This signal is digitized through an A/D converter and the resulting discrete signal is $R_{k,s}[m]$. The discrete signal $R_{k,s}[m]$ is a sequence of numbers defined for every discrete time m, where m ranges from 0 to $M-1$ (M is the total number of discrete points).

The windowed data $W_{k,s}[m]$ is defined as a portion of $R_{k,s}[m]$, with m varying from M_1 to $M_2 (M_2 < M$, and $M_2 - M_1 \leq M)$.

The time reversal version of the windowed data $W_{k,s}[m]$ represents the transmitted signal for transmission step #$(s+1)$; it is defined as follows:

$$E_{k,s+1}[m] = W_{k,s}[M_2 - m], \quad \text{with} \quad M_1 \leq m \leq M_2.$$

These operations are performed for the N elements of the array. In order to represent the contribution of the total aperture of the array, we define for reception step #s: 1) R_s as the set of the N individual received signals $R_{k,s}[m]$, and 2) W_s as the set of the N individual windowed data $W_{k,s}[m]$, and for transmission step #s, E_s as the set of the N individual transmitted signal $E_{k,s}[m]$.

C. The Experimental Procedure

The four steps required for the basic time reversal process in NDT are now presented step by step (Fig. 3).

1) Transmit Step #1: The first incident pulsed wave is transmitted from the liquid towards the solid by one (or more) element(s) of the array. In this first transmission, the array sends unfocused acoustic energy into the material.

2) Receive Step #1: The echoes coming from the block are measured by the same 2-D array on the N transducers. For each transducer k, the corresponding discrete signal $R_{k,1}[m]$ is recorded in a storage memory. If a defect is present in the illuminated volume, it behaves as an acoustic source and reflects a small amount of the energy transmitted in the previous step.

3) Transmit Step #2: During this step, we choose the origin and temporal length of the signals to be time-reversed. This is achieved through the definition of temporal windows identical for all the transducers, each window corresponds to a given depth of inspection in the material. The depth of inspection is known by measuring the transit time of the acoustic pulse as in conventional ultrasonic inspection. For each element k, the windowed signal $W_{k,1}[m]$ is time reversed and stored in the corresponding transmit memory. The new transmit signals, E_2, are used to transmit a second wave from the array toward the block.

4) Receive Step #2: The new echoes coming from the titanium sample R_2 are recorded. If the time reversal windows previously selected W_1 contains information from a defect, the resulting time reversed wave refocuses naturally on it, and the signals W_2 show a high level amplitude. The defect is now strongly amplified, it is easily detected.

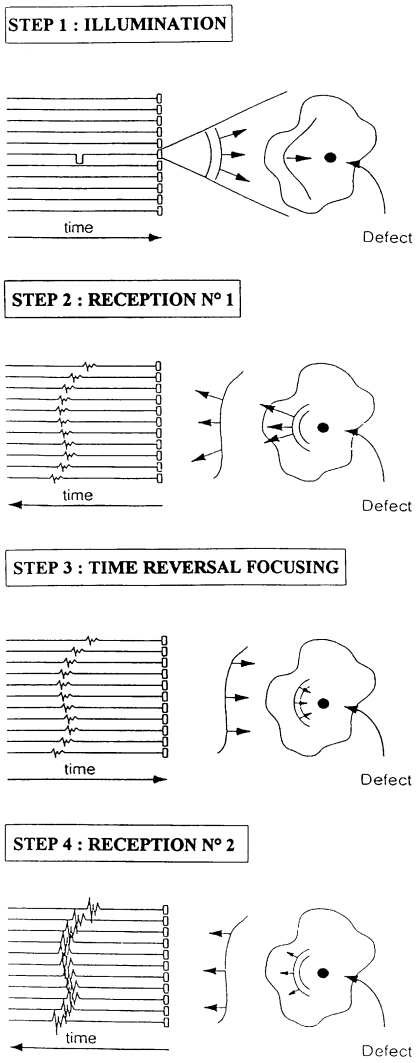

Fig. 3. Nondestructive testing with time reversal mirror.

D. Titanium Inspections Through Plane Interfaces

1) Basic Experiments: The French aircraft company S.N.E.C.M.A. made an important effort to improve ultrasonic inspection of titanium alloys. This study has been developed for four years in our laboratory [9]. In commercial titanium alloy, two kinds of "phases" of grains occur: "alpha" grains and "beta" grains. In jet engine components, both alpha and beta grains are present. During the elaboration process of titanium, metallurgical inclusion defects such as "hard-alpha" can appear. A hard-alpha inclusion is a localized region of alpha phase grains which have a substantially higher hardness and brittleness than the surrounding material. If not detected, hard-alpha inclusions can become crack initiation sites and lead to component failure. The detection sensitivity of this kind of defect is limited because titanium is an acoustically noisy medium: The strong ultrasonic speckle noise is induced by the polycrystalline microstructure. A second limitation comes from the characteristics of the hard-alpha: This defect has a low reflectivity due to a small acoustic impedance mismatch, and has irregular and unknown shape.

In the following, the time reversal process is compared for signals coming from two different zones of interest from a plane titanium sample. One zone contains a hard-alpha defect embedded in the titanium microstructure, the other contains only titanium microstructure. The experiment is carried out with the 2-D array described previously.

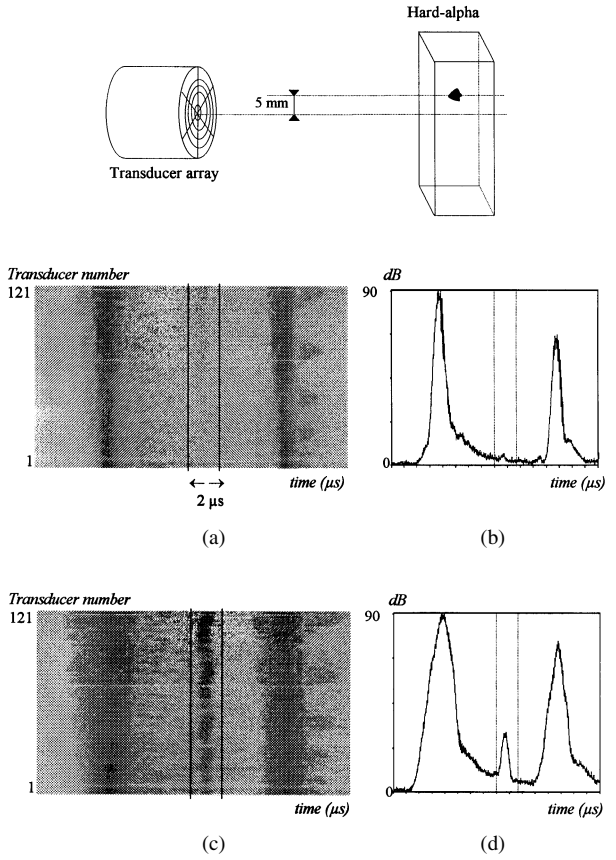

Fig. 4. Time reversal process on a zone containing a hard-alpha. (a) Grey level B-Scan presentation of reception 1. (b) Incoherent summation with logarithmic scale of reception 1. (c) Grey level B-Scan presentation of reception 2. (d) Incoherent summation with logarithmic scale of reception 2.

2) Time Reversal of Signals Coming from a Zone Containing a Hard-Alpha: An artificial hard-alpha defect is located 20 mm below the surface. A pulse echo calibration with a classical transducer shows that it corresponds to a backscattered amplitude field equivalent to a 0.4-mm diameter Flat Bottom Hole. In this experiment, the hard-alpha is located 5 mm off the symmetry axis of the array. We now present in detail the four steps needed to focus ideally on the hard-alpha.

The first incident wave is transmitted by the central element of the 2-D array. Fig. 4(a) shows the recorded data in grey level for reception 1 for the 121 elements. Data are presented in B-Scan mode, where the horizontal axis represents time (equivalent to depth) and the vertical axis represents the transducer number; they correspond to the logarithmic envelope of the echographic signals received on the 121 elements of the array. The bottom line in Fig. 4(a) is the signal from element #1, the second line from element #2, and so on. From these data, we can see the echoes coming from the front and back faces of the titanium block. Between these high amplitude echoes, we note the titanium speckle noise induced by the microstructure. This reflected sound results in a defect signal which is superimposed upon the grain noise background. Here, the defect signal can not be readily differentiated from the

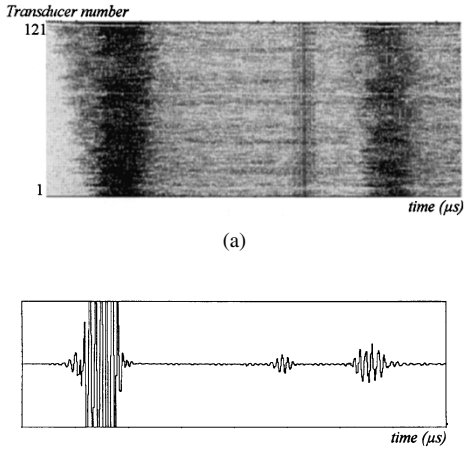

(a)

(b)

Fig. 5. Coherent summation of reception 2 with linear scale. (a) B-Scan presentation of reception 2 after shifting the signals. (b) Coherent summation.

noise background. The fraction of the incident sound reflected depends on the magnitude and abruptness of the impedance contrast, and on the size and shape of the defect.

In the second step, a 2-μs (6 mm of titanium) time window is chosen after the front face echo, selecting a titanium section which origin is located at a depth of 20 mm.

In the third step, the windowed data are time reversed and retransmitted. After propagation, the time reversed wave focuses on the hard-alpha.

In the last step, we record the echoes coming from the block, the corresponding data are shown in Fig. 4(c). The echoes from the interfaces still exist, but between them an oscillating line clearly appears. This line corresponds to the echoes from the hard-alpha received by the elements of the array. The defect signal can be readily differentiated from the noise background and the defect is detected. After a time reversal process, the signal-to-noise ratio increases. The amplitude and oscillation correspond to an off-axis defect, whose wavefront intercepts the 2-D array obliquely. The technique is efficient whatever the position of the defect in the incident beam. The TRM performs in real time, a Fermat's surface matched to the relative positions between the TRM and the defect. The hard-alpha defect is automatically detected in a section of more than 1 cm^2 around the axis of the 2-D TRM.

A more compact presentation of the time reversal process can be implemented by adding the 121 logarithmic envelopes of the received signals (Fig. 4(b) and (d)). This sum generates a single array output. In the following, this process is called "*incoherent summation*" because the individual data are not in phase. The incoherent summation for reception step #s, Inc_s is determined according to the discrete summation

$$Inc_s[m] = \sum_{k=1}^{N} \mathrm{Log}(R_{k,s}[m]) \qquad 0 \leq m < M.$$

The logarithmic scale dynamic is 90 dB. Looking at this incoherent summation Inc_2 (Fig. 4(d)), we note that the amplitude of the defect is now 20 dB over the noise level. This summation can be implemented easily, but it is not an optimal processing because the received signals are not in phase.

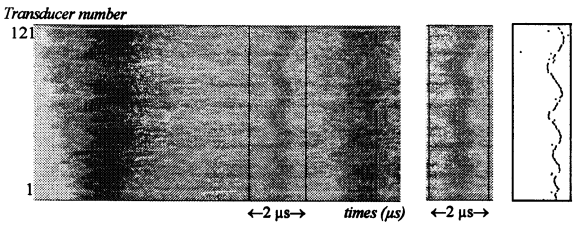

(a) (b) (c)

Fig. 6. Fermat's surface at reception 2. (a) B-Scan presentation of reception 2. (b) Time reversal window. (c) Fermat's surface.

The total output signal can be improved significantly by correcting the individual signals for the differences in arrival times. A summation of the shifted individual signals is performed to obtain a single combined signal for the array. Such a time compensating process corresponds to a *coherent summation* and allows the echo level to be increased.

A cross-correlation algorithm can be used to determine the time shifts between the individual echoes [10]. This algorithm presents two drawbacks: it requires that all of the individual signals be stored and it is time consuming. We have developed a simpler and quicker algorithm to measure the time delays. This algorithm needs a complete time reversal sequence and uses the symmetrization property of the time reversal process. Indeed, we observe that, after one time reversal process, the received signals on the array are symmetrical. This symmetrization property is due to the fact that a time reversal process is equivalent to a matched filter [6]. From this property, the time delays are determined by finding on each element k the position of the peak amplitude $p_{k,2}$ of the symmetric received signal $W_{k,2}[m]$. As the signal becomes symmetric after one time reversal process, the location of the maximum pressure becomes precise and easy. This algorithm is simpler and quicker than the cross-correlation method; it only needs to store the positions of the maximum pressure.

The coherent summation is much more efficient than the incoherent one. If $p_{k,s}$ represents the position of the maximum of the signal $W_{k,s}[m]$, the coherent summation for reception step #s, Coh_s is determined according to the discrete summation

$$Coh_s[m] = \sum_{k=1}^{N} R_{k,s}[m - p_{k,s}] \qquad 0 \leq m < M.$$

Fig. 5 presents the coherent summation Coh_2 in a linear scale, the signal-to-noise ratio reaches 30 dB. We note that the echo from the hard-alpha reaches a level comparable to the one of the back face of the titanium sample.

The location of the 121 maxima $p_{k,2}$ (Fig. 6(c)) allows us to determine a curve that represents an ideal wavefront coming from the defect. Such a wavefront is a very good approximation of the Fermat's surface required to refocus on the defect from the transducer array (Fig. 6). The Fermat's surface obtained in this way (Fig. 6(c)) shows a continuous aspect.

3) Time Reversal of Signals Coming from a Speckle Noise Zone: In the second part of the experiment, the time reversal process is now evaluated with a time reversal window located in a pure speckle noise zone. Fig. 7(c) shows that the signal behavior does not change after one time reversal process. We

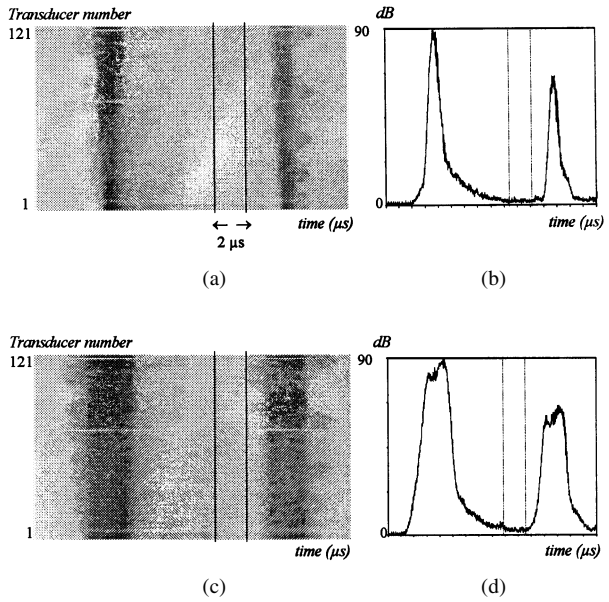

Fig. 7. Time reversal process on a zone containing pure speckle noise. (a) Grey level B-Scan presentation of reception 1. (b) Incoherent summation with logarithmic scale of reception 1. (c) Grey level B-Scan presentation of reception 2. (d) Incoherent summation with logarithmic scale of reception 2.

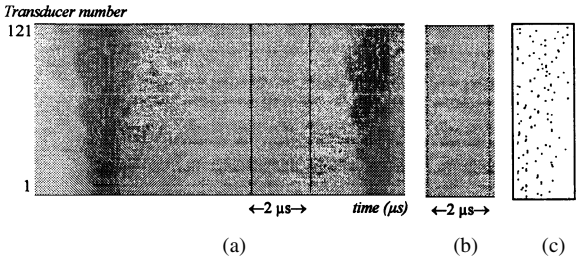

Fig. 8. Fermat's surface at reception 2. (a) B-Scan presentation of reception 2. (b) Time reversal window. (c) Fermat's surface.

do not observe any wavefront appearing in the data. This is a different behavior of time reversal on echographic speckle noise compared with hard-alpha signals. In titanium, the speckle noise comes from the microstructure whose dimension (a few μm) is small compared to the wavelength (1.2 mm for longitudinal waves). The time reversal process cannot refocus the energy on the acoustic source of the speckle noise. This is due to the loss of information on the small details of the titanium microstructure during propagation of the backscattered wave with a 5-MHz center frequency.

No peak arises from the incoherent summation of the 121 received signals Inc_2: they are completely uncorrelated (Fig. 7(b)). If we calculate the 121 maxima $p_{k,2}$, we note that it differs completely from one element to another (Fig. 8(c)). The Fermat's surface obtained in this way (Fig. 8(c)) shows a random aspect. Now, if all this data is added with the coherent summation technique, Coh_2 shows a peak amplitude that can be considered as an artifact (Fig. 9(b)) resulting from an alignment of the maximum of the individual speckle noise signals. Such a process clearly amplifies the speckle noise through a coherent summation.

In summary, the coherent summation is optimal if there is a defect in the zone of interest, and incoherent summation is optimal in speckle noise zone.

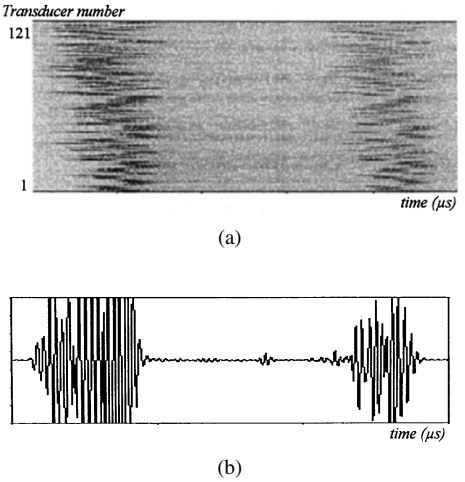

Fig. 9. Coherent summation of reception 2 with linear scale. (a) B-Scan presentation of reception 2 after shifting the signals. (b) Coherent summation.

In this section, we show the difference in behavior of the time reversal process depending on whether the backscattered signals come from a coherent or incoherent source. As previously observed, the origin of the backscattered signals can be found by analyzing the Fermat's surface shape. Indeed, in the case of a coherent source, the calculated Fermat's surface is continuous, and in the case of a incoherent source, the Fermat's surface is discontinuous. It is judicious to use this difference of behavior to recognize the continuous Fermat's surface, and calculate, in this case only, the coherent summation. This difference can be pointed out by computing an algorithm able to determine if a curve is continuous or not. Such an algorithm needs to calculate the discrete time shift between elements k and $k+1$, and then decide if such a time shift is linked to the path differences between the defect and the individual elements. The discrete time shift is defined as the difference between $p_{k,2}$ and $p_{k+1,2}$.

To decide if the time shift is correct and corresponds to the path difference between the defect and the individual elements of the array, knowledge of many parameters, such as the velocity of the waves in the two propagating media, the distance between adjacent transducers, the shape of the transducers, and also the position of the defect with respect to the 2-D array, is required. Such an algorithm is time-consuming and difficult to implement. After one time reversal, a simple trade-off consists in using only incoherent summation for all the inspections.

With the iterative mode of the time reversal method, a new algorithm is presented to determine the nature of the acoustic source (defect or speckle noise) without knowing the acoustic parameters of the propagating media, nor the position of the array with respect to the block. Indeed, better processing can be performed if we carefully analyze at least two consecutive iterations of the time reversal process.

IV. The Iterative Technique

In the case of a defect signal of low amplitude, multiple iterations can be implemented to improve the ability to focus on the defect, and thus increase the signal-to-noise ratio. The

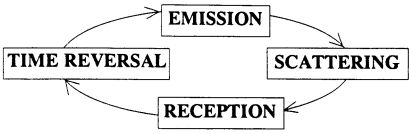

Fig. 10. Iterative mode loop.

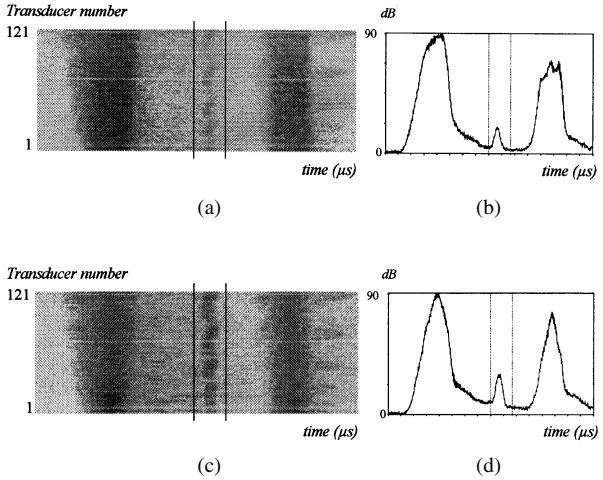

Fig. 11. Iterative time reversal process on a zone containing a defect. (a) Grey level B-Scan presentation of reception 2. (b) Incoherent summation of reception 2. (c) Grey level B-Scan presentation of reception 3. (d) Incoherent summation of reception 3.

iterative time reversal mode can also be used to distinguish between speckle and defects.

To iterate the process, we start from reception 2. At this step, we define for each element k the new time reversal window $W_{k,2}[m]$. These windowed data are time reversed and stored in the corresponding transmit memory. The resulting emission, E_3, can be considered as the emitted wave of the next time reversal iteration. The operation can be repeated in an iterative loop, as shown schematically in Fig. 10; this describes the iterative time reversal process.

Experimentally, we perform two iterative loops: a new time reversal operation is processed after reception 2, and new data from the medium are recorded during reception 3, R_3. We illustrate the results of the iterative time reversal operation for a zone containing a small defect and a zone containing only speckle noise.

A. Iterative Process for a Zone Containing a Hard-Alpha

In Fig. 11(a) and (c), we observe that the signals received after one and two time reversal operations, W_2 and W_3, are similar and show an identical wavefront. Fig. 11(b) and (d) shows the incoherent summation Inc_2 and Inc_3. Fig. 12 represents the temporal signals received on transducer $k, W_{k,2}[m]$ (solid line) and $W_{k,3}[m]$ (dotted line). They are very similar up to an amplitude factor due to the amplification efficiency of the time reversal process. This result is linked to the fact that the echographic signals come from a coherent source of small dimension (the hard-alpha). We also note that the two waveforms are symmetric.

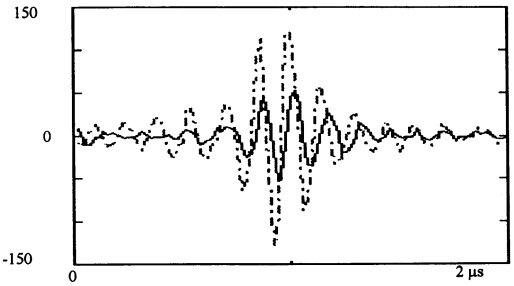

Fig. 12. Echoes of the hard-alpha after one (solid line) and two (dotted line) time reversal process.

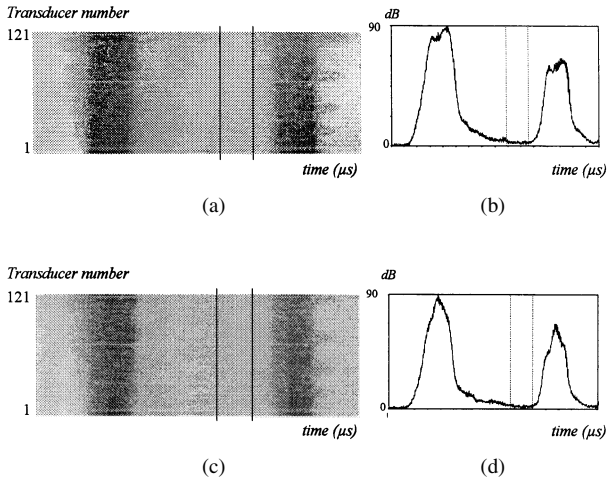

Fig. 13. Iterative time reversal process on a pure speckle noise zone. (a) Grey level B-Scan presentation of reception 2. (b) Incoherent summation of reception 2. (c) Grey level B-Scan presentation of reception 3. (d) Incoherent summation of reception 3.

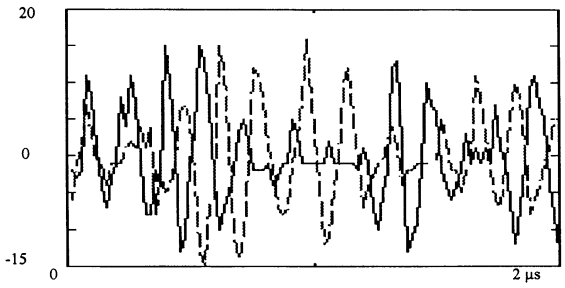

Fig. 14. Echoes of the speckle noise after one (solid line) and two (dotted line) time reversal process.

B. Iterative Process on a Pure Speckle Noise Zone

If the echoes come from a pure speckle noise zone (Fig. 13), a careful analysis of the signals W_2 and W_3 show that they are random and completely uncorrelated. Fig. 14 shows two waveforms received at receptions 2 (solid line) and 3 (dotted line) on the same transducer that was used to detect the signal shown in Fig. 12. We note that the two signals show quick variations and seem to be random signals. The two waveforms are uncorrelated and there is no amplification in this process. The time reversal has lost the information required to refocus on the small details of the microstructure, so there is no focusing effect.

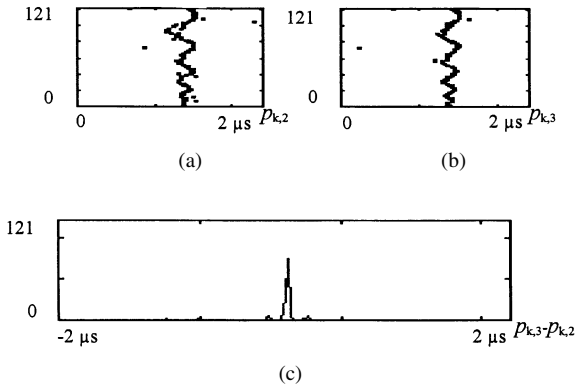

Fig. 15. Deviation histogram on a zone containing a defect. (a) Fermat's surface of reception 2. (b) Fermat's surface of reception 3. (c) Deviation histogram.

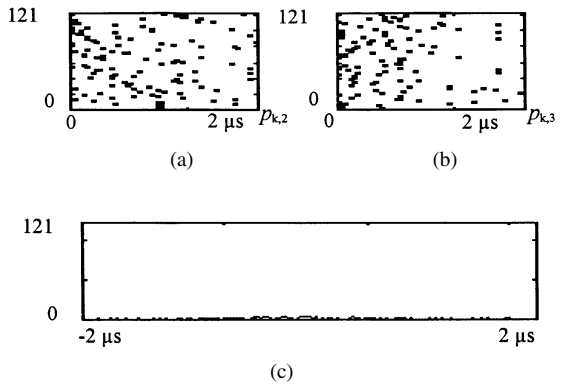

Fig. 16. Deviation histogram on a zone containing a pure speckle noise. (a) Fermat's surface of reception 2. (b) Fermat's surface or reception 3. (c) Deviation histogram.

C. Comments

The iterative time reversal process appears to be an interesting tool for the inspection of noisy background media like titanium blocks for two reasons. First, this technique behaves differently depending on whether the inspection zone is coherent or not. This allows it to distinguish a defect from the surrounding material. Second, it improves the detection of small defects by increasing the signal-to-noise ratio.

When an iterative time reversal process is performed on a defect zone, the resulting wavefronts W_2 and W_3 are similar, up to an amplitude factor. These results can be explained as follows. After the first time reversal process, the transmission of E_2 by the 2-D array yields a convergent wave that reaches the defect zone. As the dimension of the defect is small compared to the wavelength, it generates a quasi-spherical reflected wave. The shape of the corresponding received wavefront W_2 results from the intersection of this wave with the surface of the 2-D array. The time delay law obtained by the Fermat's surface technique depends only on the position of the defect with respect to the interface and the array and results from the path length covered by the wave from the defect to each element. In the second time reversal process, the transmission of E_3 yields a new focused wave on the same defect. The defect again generates a quasi-identical reflected wave that reaches the surface of the 2-D array. The time delay law obtained from the new received signals, W_3, results from the same path length covered by the wave from the defect to each element as during the previous iteration. After one or two time reversal operations, the illuminated zone is reduced to the dimensions of the diffraction limited focal spot. The echoes measured by the 2-D array after one or two iterations come from the same zone of the material (the defect). Although they have the same shape, their amplitudes can increase until the focal spot is reduced to the diffraction limit.

When the iterative time reversal process is performed on a speckle noise zone, the resulting wavefronts W_2 and W_3 are different. To understand these results, we recall how the microstructural noise is generated. In a metal grain, the speed of sound depends upon the direction of propagation relative to the crystal lattice. Because the crystal lattices of two adjacent grains are usually not aligned with one another, there is a velocity and impedance contrast at a grain boundary. The reflected waves from the various grain boundaries encountered by the beam backpropagate in the direction of the 2-D array, resulting in the microstructural noise. The microstructural noise depends upon the number of grains, as well as the relative position of the grains with respect to the acoustic beam [11]. The signal observed at a specific transducer depends upon the interference pattern that is fully deterministic and only depends upon the relative position of the grains and the 2-D array. If the illumination or detection conditions change, the measured signal changes.

For the iterative time reversal process, W_2 and W_3 are different because the illumination conditions are different. Indeed, the first emitted wave is generated by the central element and the second one is generated by the 121 transducers simultaneously. Since the illumination conditions are different, the signals W_1 and W_2 are necessarily different, which makes the corresponding time reversal versions of the transmitted signals E_2 and E_3 different, too. Therefore, the received signals W_2 and W_3 must differ.

The iterative time reversal technique can distinguish between a coherent and an incoherent backscattered field. Using this feature of the time reversal process, we developed a new signal processing technique to detect a defect in the speckle noise: the time reversal deviation histogram [9].

V. The Time Reversal Deviation Histogram Technique

This technique is based on the evaluation of the degree of similarity of the received wavefront after one or two time reversal operations.

A simple approach consists of the computation of a normalized correlation coefficient between the different signals inside the time-reversed windows for receptions 2 and 3. The coefficient is determined by evaluating the peak value of the discrete expression $c[n]$

$$c[n] = \frac{\sum_{k=1}^{121} \sum_{m=M_1}^{M_2} W_{k,2}[m] \times W_{k,3}[m-n]}{\sum_{k=1}^{121} \left[\sum_{m=M_1}^{M_2} (W_{k,2}[m])^2 \times \sum_{m=M_1}^{M_2} (W_{k,3}[m])^2 \right]^{1/2}}.$$

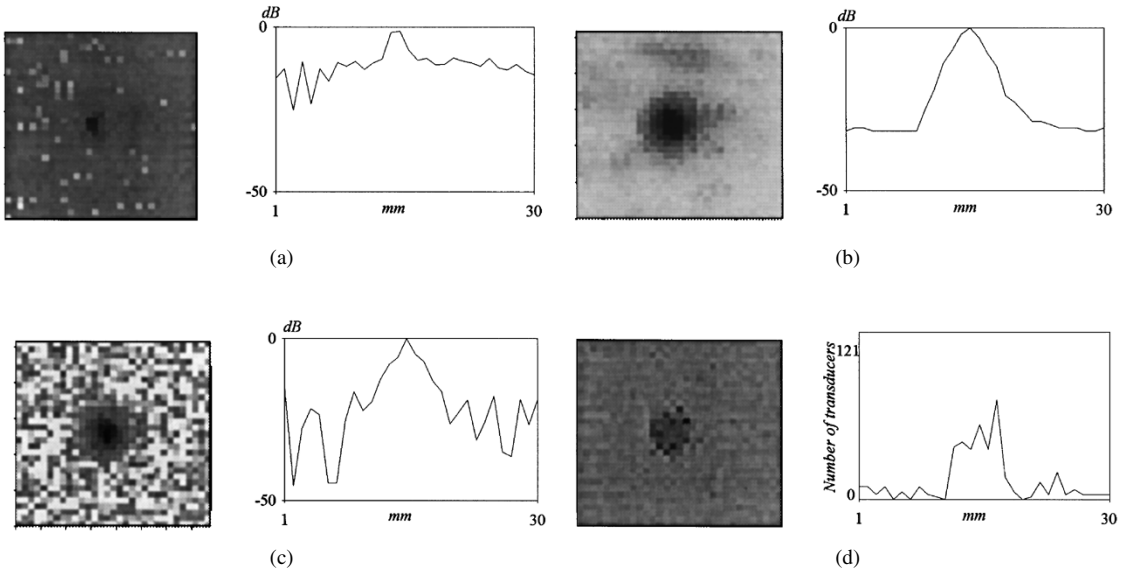

Fig. 17. Comparison of conventional technique and time reversal techniques for the detection of a 0.4-mm flat bottom hole embedded at 65-mm depth in a noisy background titanium component. (a) Conventional technique. (b) Time reversal incoherent summation. (c) Time reversal coherent summation. (d) Time reversal deviation histogram.

If W_2 and W_3 are those represented in Fig. 11(a) and (c), this coefficient is close to 0.8. In the speckle noise zone (Fig. 13(a) and (c)), the correlation coefficient decreases to 0.2. This technique is time-consuming since it requires that the 121 signals (W_2 and W_3) be stored before proceeding with the cross-correlation. Thus, we have developed a much simpler approach using the concept of Fermat's surface previously presented. The new algorithm compares the Fermat's surfaces obtained after one and two time reversal operations.

For a zone containing a hard-alpha, the two Fermat's surfaces corresponding to Fig. 11(a) and (b) are plotted on Fig. 15(a) and (b). The vertical axis represents the transducer number and the horizontal axis the values $p_{k,2}$ and $p_{k,3}$. For each element k, the deviation (or difference) between $p_{k,2}$ and $p_{k,3}$ is calculated and noted p_k and the resulting data are represented through a histogram (Fig. 15(c)). The horizontal axis represents p_k and the vertical axis of the histogram represents the number of transducers. If the length of the time reversal window is M, then the horizontal range of the deviation histogram is between $-M$ and $+M$. If the 121 values of $p_{k,2}$ and $p_{k,3}$ are similar, the resulting deviation histogram shows a peak amplitude near $p_k = 0$. In the experiment presented above, the maximum of the deviation histogram reaches 90 transducers (Fig. 15(c)) for a zone containing a defect. This means that 90 transducers present the same time shift after one and two time reversal operations.

When the iterative time reversal process is performed on a pure speckle noise zone, the two Fermat's surfaces are different. Fig. 16(a) and (b) represents $p_{k,2}$ and $p_{k,3}$, corresponding to Fig. 13(a) and (b). The two curves are uncorrellated. Therefore, the values of the deviation p_k are spread on a large range between between $-M$ and $+M$ and the deviation histogram is flat, without any maximum (Fig. 16(c)).

The two techniques, normalized correlation coefficient and deviation histogram, can be compared. A normalized correlation coefficient $c[n]$ close to one corresponds to a deviation histogram with a high amplitude narrow peak whose value is near the total number of transducers (Fig. 15(c)). A normalized correlation coefficient $c[n]$ close to zero corresponds to a spread deviation histogram whose peak value is very low (Fig 16(c)). Defining a detection threshold, this allows a speckle noise zone to be distinguished from a defect zone.

VI. C-Scan Imaging with Time Reversal Mirror

We have described three different time reversal procedures that can be applied to the defect detection in titanium: incoherent summation, coherent summation, and the deviation histogram. In Fig. 17, a comparison between these three techniques and the classical electronic focusing method is presented with C-Scan images.

A. Principle of Ultrasonic Field Imaging System

The experiments are carried out using the time reversal prototype and the 2-D array described above. The 2-D array is mounted on a vertical axis (Z-axis) with two lateral degrees of freedom (X-axis and Y-axis). The vertical axis was in turn attached to a bridge allowing motor-controlled translation motion in the two lateral dimensions. The lateral position of the 2-D array above the specimen is under computer control for the scanning operations. The waterpath is defined by observing the propagation time of the front surface echo. Once this parameter is fixed, the 2-D array is moved above the specimen in both the X and Y directions. In our experiment, the waterpath is 70 mm, such that the focal spot is located near the defect.

In the classical electronic focusing method, the entire array aperture works in parallel, both in transmit and receive modes,

to achieve focusing at the geometrical focus of the 2-D array (330 mm of water). At each position of the array, the 121 received signals are summed. To obtain the C-Scan image, we only report the maximum of this resulting signal.

Using the Time Reversal Mirror, only one datum is recorded for each position of the 2-D array in front of the solid, as in the case of a classical C-Scan. The datum can be the maximum of: 1) the incoherent summation, 2) the coherent summation, or 3) the deviation histogram. C-Scan imaging is achieved in real time with the TRM.

The results presented in this paper are obtained with a very noisy forged titanium sample, where a 0.4-mm diameter flat bottom hole is located at a depth of 65 mm. The scanning is performed over a 30×30 mm^2 area around the position of the defect, with a 1-mm spatial resolution. In Fig. 17, to the right of each image, a specific line of each C-Scan is presented in order to evaluate the signal to noise ratio.

B. Results

The results confirm the effectiveness of the time reversal technique, especially the incoherent summation (Fig. 17(b)) and the deviation histogram (Fig. 17(d)). Compared to the conventional technique (Fig. 17(a)), a significant speckle noise reduction can be achieved with these two time reversal techniques.

Using the classical focusing technique, the signal-to-noise ratio reaches 13 dB and the defect is detected only in a very small zone (Fig. 17(a)). The time reversal techniques allow detection of the defect in a larger zone (1 cm^2) with a high signal-to-noise ratio. The incoherent summation (Fig. 17(b)) presents the highest signal-to-noise ratio, 30 dB. Note that the incoherent summation increases the apparent size of the defect. The -10 dB width appears to be 1.4 mm in Fig. 17(a), whereas the -10 dB width appears to be about 3 mm in Fig. 17(b). For the coherent summation (Fig. 17(c)), the signal-to noise ratio is reduced to 15 dB (this technique amplifies the speckle noise). The results of the C-Scan obtained with the time reversal deviation histogram are shown in Fig. 17(d). Unlike the previous images, this C-Scan cannot be interpreted in a dB scale. At the position of the defect, the maximum is close to 70 transducers and for the speckle noise the maximum is only eight transducers.

When using the classical focusing inspection method, the first transmitted wave is identical for all the scanning. For each position of the transducer array, a focused wave is transmitted in the material, whatever the zone of inspection. If this zone contains a defect or only speckle noise, it receives the same energy. In a pure speckle noise zone, the backscattered signal can be very high and the focusing step, also used in the receive mode, increases the noise level. On the contrary, time reversal behaves differently depending on the kind of the backscattered source. In the case of a pure speckle noise source, the time reversal process generates an unfocused wave in the material, thus resulting in a small acoustic energy on the speckle noise source. In the case of a defect, all the acoustic energy of the system is focused on it, therefore increasing the signal-to-noise ratio.

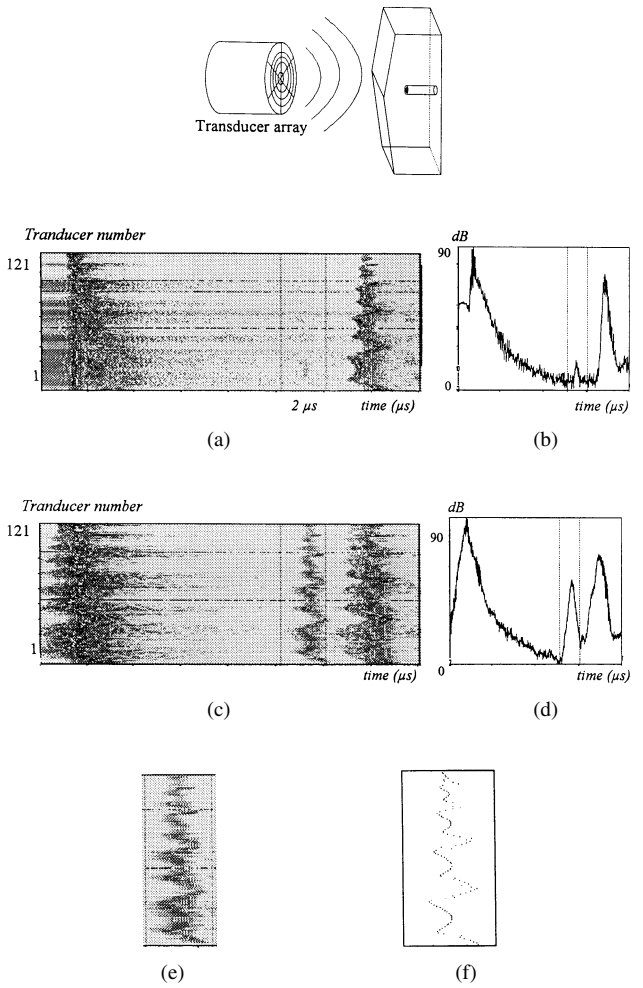

Fig. 18. Time reversal on sample with complex shape. (a) Grey level B-Scan presentation of reception 1. (b) Incoherent summation with logarithmic scale of reception 1. (c) Grey level B-Scan presentation of reception 2. (d) Incoherent summation with logarithmic scale of reception 2. (e) Time reversal window. (f) Fermat's surface.

When using the classical focusing technique, the zone of detection of a small defect depends upon the dimensions of the focal spot. With the time reversal process, a small defect can be detected in a wide zone. The dimension of this zone is related to the dimension of the first incident field. When the sample of interest has only one defect, the broadening of the detection zone can be very useful. It allows, in the inspection process, larger steps in the lateral scanning dimensions. However, when two or more small defects are close together, the time reversal process cannot simply distinguish between these defects and more iteration steps are required to focus the ultrasonic field on the larger defect [5].

VII. Inspections Through Complex Interface

In this section, we analyze the effectiveness of the time reversal technique in detecting a defect located beneath a prismatic interface. This defect is a 2-mm diameter flat bottom hole drilled in a duralumin block, so that its bottom is located 40 mm below the prismatic angle of the block. The array transducer is positioned over the prismatic angle. For the

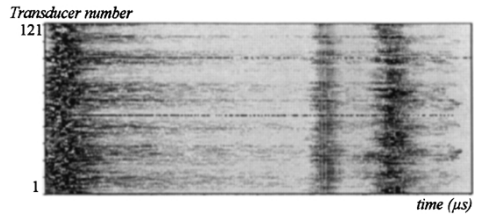

(a)

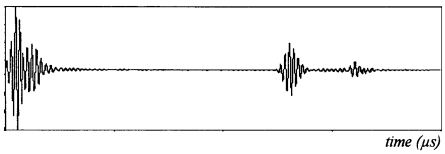

(b)

Fig. 19. Coherent summation of reception 2. (a) B-Scan presentation of reception 2 after shifting the signals. (b) Coherent summation.

first step, only the central element transmits a pulse wave towards the solid in order to generate unfocused acoustic energy into the material. Waveforms are then recorded from all 121 elements of the array transducer. We note in the B-Scan presentation of the received signal R_1 (Fig. 18(a)) the complex shape of the front and back face echoes of the block. We also note that only a few transducer elements receive enough energy from the defect to be detectable. The first incoherent summation Inc_1 (Fig. 18(b)) presents a peak amplitude which is only 2 dB over the background noise level.

We choose for the experiment a time reversal window of 2-μs duration. The signals included in the time reversal window are time-reversed and retransmitted towards the material. Fig. 18(c) shows the resultant B-Scan image after one time reversal operation. The B-Scan presentation of the received signal R_2 shows a complex wavefront that corresponds to the echo from the defect. After one time reversal operation, the signal-to-noise ratio grows significantly and the defect is easily detected. The incoherent summation Inc_2 (Fig. 18(d)) has a 30-dB signal-to-noise ratio. To improve this signal-to-noise ratio, the coherent summation can also be processed. Fig. 18(f) shows the Fermat's surface obtained from the complex wavefront recorded in the selected window on Fig. 18(c). It represents the values $p_{k,2}$ corresponding to Fig. 18(e). The received signals of Fig. 18(c) are then shifted according to these values in order to get all their maxima at the same time (Fig. 19(a)). The linear coherent summation Coh_2 (Fig. 19(b)) gives an excellent result, the defect signal has now a greater amplitude than the back face echo (10 dB), and it results in a 50-dB signal-to-noise ratio.

VIII. Conclusions

TRM represents a real improvement in inspection of samples with high ultrasonic speckle noise level. All the experiments show the effectiveness of the time reversal technique in locating a defect within a component that has a plane or a complex interface. With this technique, the signal-to-noise ratio is improved for two reasons. First, the time reversal process is a self-adaptive focusing technique that creates a focused wave matched to the defect shape, to the propagation medium, and to the geometry of the mirror and the medium. Second, the time reversal process reduces the amplitude of the speckle noise. Due to the loss of information during the propagation, the process cannot focus on microstructure whose dimension is small compared to the wavelength.

The first experiments performed with the time reversal mirror prototype working at 5 MHz allow the detection of a 0.4-mm flat bottom hole located at 65-mm depth in a noisy forged component of titanium. The signal-to-noise ratio reaches 30 dB. In another experiment, we demonstrate the ability of the time reversal process to detect a small defect located beneath an interface with a complex geometry.

While using the time reversal process, C-scan images can be realized in real time. In our system, controlled by a DSP unit, a complete time reversal sequence (three iterations) and signal processing (incoherent summation, coherent summation, and deviation histogram) requires about 40 ms. These results show the potential of time reversal to be adapted and used for various industrial problems.

Acknowledgment

The authors wish to express their gratitude to Dr. D. Cassereau for helpful assistance in this paper.

References

[1] O. T. von Ramm and S. W. Smith, "Beam steering with linear arrays," *IEEE Trans. Biomed. Eng.,* vol. BME-30, pp. 438–452, 1983.

[2] D. H. Turnbull and F. S. Foster, "Beam steering with pulsed two-dimensional transducer arrays," *IEEE Trans. Ultrason., Ferroelec., Freq. Contr.,* vol. 38, pp. 320–333, 1991.

[3] S. W. Smith, H. G. Pavy, and O. T. von Ramm, "High-speed ultrasound volumetric imaging system—Part 1: Transducer design and beam steering," *IEEE Trans. Ultrason., Ferroelec., Freq. Contr.,* vol. 39, pp. 555–566, 1992.

[4] M. Fink, C. Prada, F. Wu, and D. Cassereau, "Self focusing with time reversal mirror in inhomogeneous media," in *Proc. IEEE Ultrason. Symp.,* Montreal, P.Q., Canada, vol. 2, pp. 681–686, 1989.

[5] C. Prada, F. Wu, and M. Fink, "The iterative time reversal mirror: A solution to self focusing in pulse-echo mode," *J. Acoust. Soc. Amer.,* July 1991.

[6] M. Fink, "Time reversal of ultrasonic fields—Part I: Basic principles," *IEEE Trans. Ultrason., Ferroelec., Freq. Contr.,* vol. 39, no. 5, Sept. 1992.

[7] F. Wu, J. L. Thomas, and M. Fink, "Time reversal of ultrasonic fields—Part II: Experimental results," *IEEE Trans. Ultrason., Ferroelec., Freq. Contr.,* vol. 39, no. 5, Sept. 1992.

[8] D. Cassereau and M. Fink, "Time reversal of ultrasonic fields—Part III: Theory of the closed time reversal cavity," *IEEE Trans. Ultrason., Ferroelec., Freq. Contr.,* vol. 39, pp. 579–592, 1992.

[9] N. Chakroun, M. Fink, and F. Wu, "Ultrasonic non destructive testing with time reversal mirrors," in *Proc. IEEE Ultrason. Symp.,* Tucson, vol. 2, pp. 809–814, 1992.

[10] S. W Flax and M. O'Donnell, "Phase-aberration correction using signals from point reflectors and diffuse scatterers: Basic principles," *IEEE Trans. Ultrason., Ferroelec., Freq. Contr.,* vol. UFFC-35, pp. 758–767, 1988.

[11] F. J. Margetan and R. B Thompson, "Microstructural noise in titanium alloys and its influence on the detectability of hard-alpha inclusions," in *Review of Progress in Quantitative NDE,* vol. 12B, D. O. Thompson and D. E. Chimenti, Eds. New York: Plenum, 1992, pp. 1717–1724.

Najet Chakroun was born in 1966 in Tunis, Tunisia. She received the D.E.A. degree in acoustic physics in 1990 from Paris VII University, Paris, France. She is currently working toward the thèse 3ème cycle from Paris VII University with S.N.E.C.M.A., the French engine aircraft company in the Laboratoire Ondes et Acoustique.

Mathias A. Fink, for photograph and biography, see p. 988 of this issue of this TRANSACTIONS.

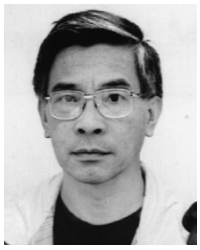

François Wu was born in 1940 in Paris, France. He received the D.E.A. degree in electronique et traitement de l'information in 1966 and the Doctorat ès-Sciences degree in physics in 1982 from Paris XI University, Orsay, France.

From 1967–1986, he worked in the Laboratory of Cristallographie et Physique des Matériaux of Prof. P. Pério at Orsay University. He was first Teaching Assistant of Cristallography and then Maitre de Conférences of Physics at Paris XI University, Orsay. Since 1987, he has been in the Laboratoire Ondes et Acoustique, Paris 7 University, Paris, France, directed by Prof. M. A. Fink. His research activities are in the development of ultrasonic time reversal mirrors for medical applications of focusing in inhomogeneous media and nondestructive control of solid materials.